Electronic Supplementary Information

An Iron-based Polyanionic Cathode for Potassium Storage with High Capacity and Excellent Cycling Stability

Haiyan He[a,b,1], Wenjiao Yao[a,1], Sarayut Tunmee[c,1], Xiaolong Zhou[a], Bifa Ji[a,d], Nanzhong Wu[a,d], Tianyi Song[a,b], Pinit Kidkhunthod[c], Yongbing Tang[a,*]

a. Functional Thin Films Research Center, Shenzhen Institutes of Advanced Technology, Chinese Academy of Sciences, Shenzhen 518055, China
b. Nano Science and Technology Institute, University of Science and Technology of China, Suzhou 215123, China
c. Synchrotron Light Research Institute, Nakhon Ratchasima 30000, Thailand
d. University of Chinese Academy of Sciences, Beijing 100049, China

 Corresponding authors.
E-mail addresses: *tangyb@siat.ac.cn*

[1] H.Y. He, W.J. Yao and S. Tunmee contributed equally to this work.

Table of contents

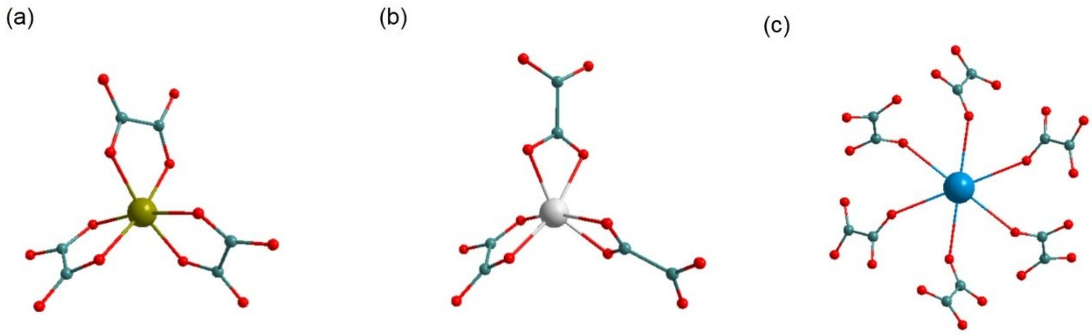

Fig. S1. Coordination of (a) Fe, (b) Li, and (c) K in KLFO.

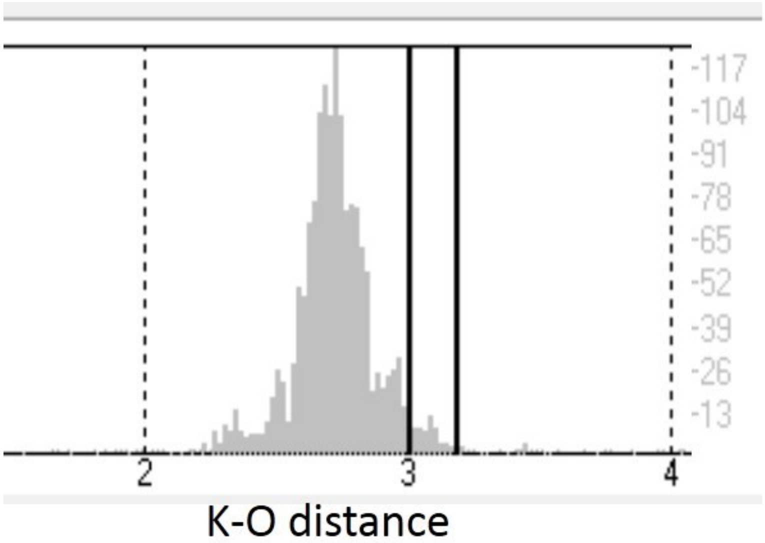

Fig. S2. K-O distance in KLFO in comparison with statistic values. Gray: 1681 compounds from statistic. Black: KLFO.

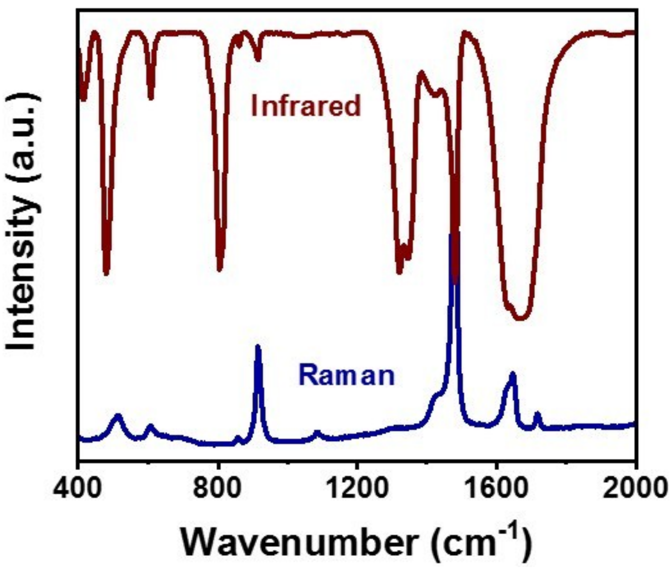

Fig. S3. FT-IR and Raman spectra of pristine KLFO sample.

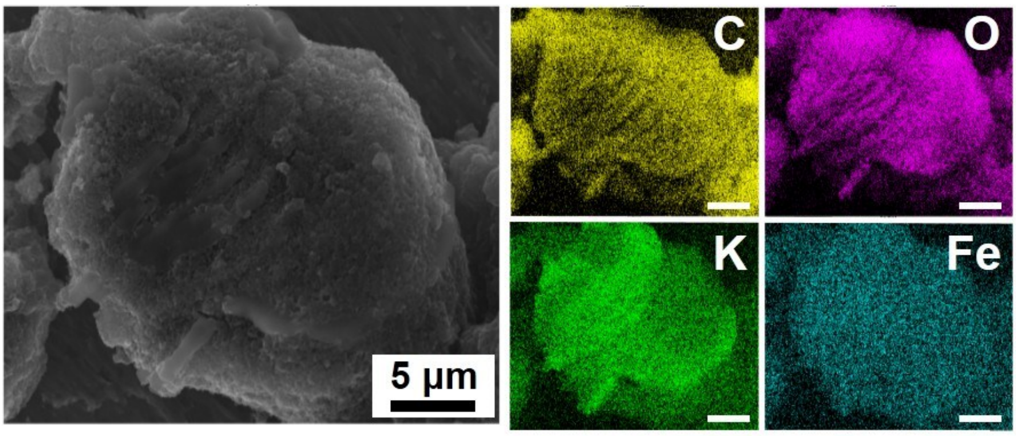

Fig. S4. SEM and EDS mapping of KLFO@C.

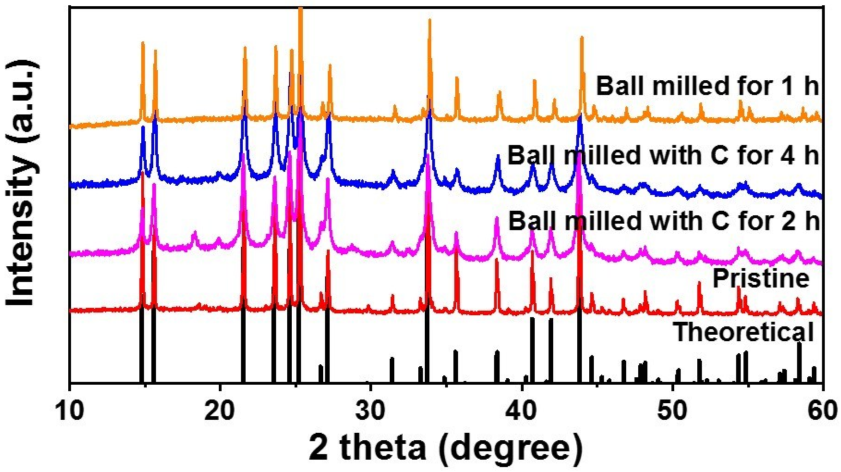

Fig. S5. Powder XRD patterns of samples at different stages.

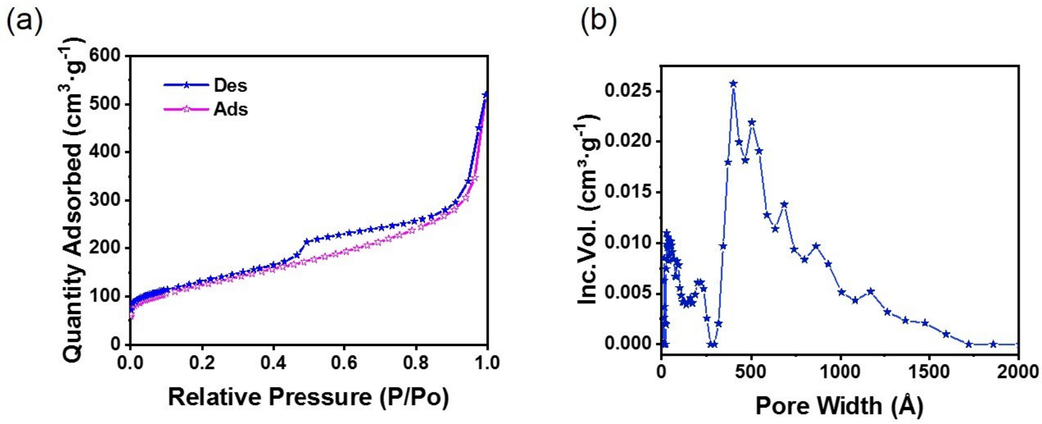

Fig. S6. Brunauer–Emmett–Teller surface area and pore structure of KLFO@C sample.

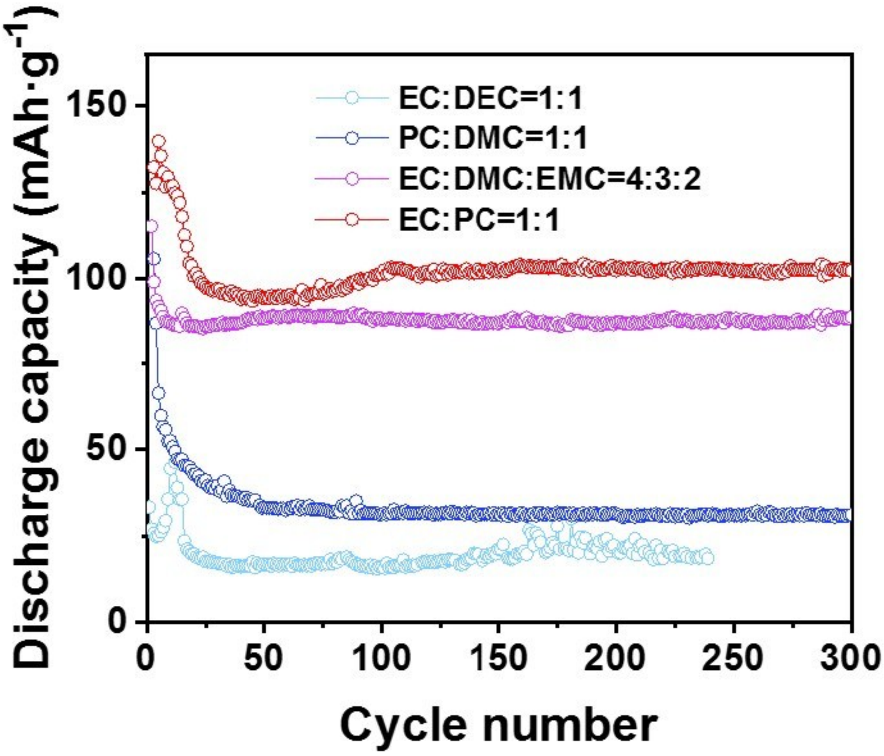

Fig. S7. Capacity retention of cells in preliminary electrolyte screening.

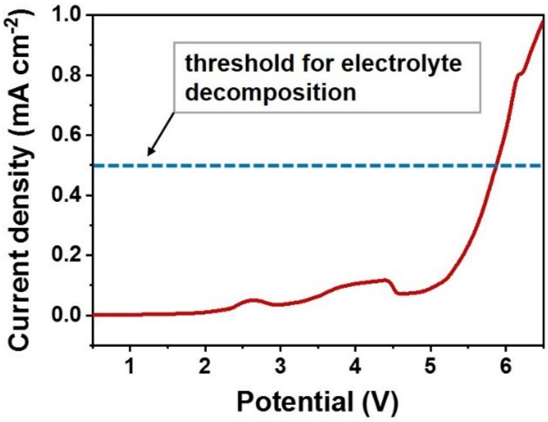

Fig. S8. Linear sweep voltammetry of the pure electrolyte cell.

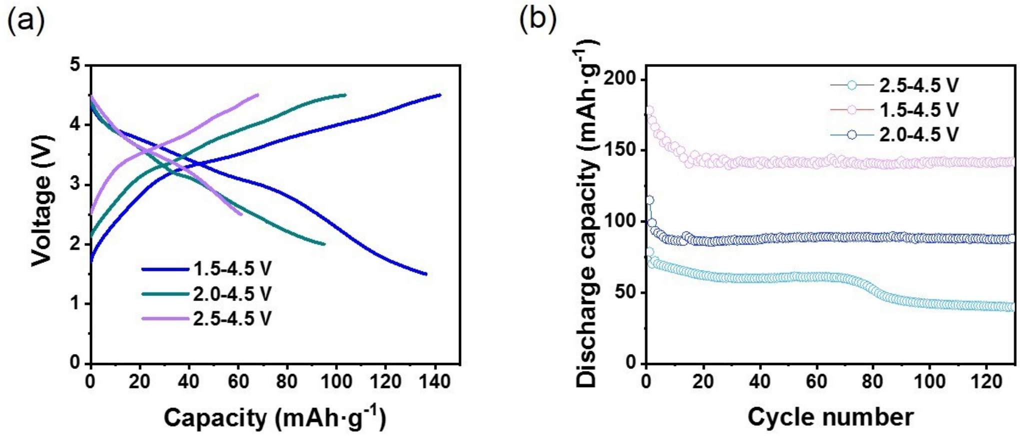

Fig. S9. Galvonostatic charging and discharging curves (a) and cycle stability (b) in different voltage windows of 2.5-4.5 V, 2.0-4.5 V and 1.5-4.5 V under the current density of 120 mA g^{-1}.

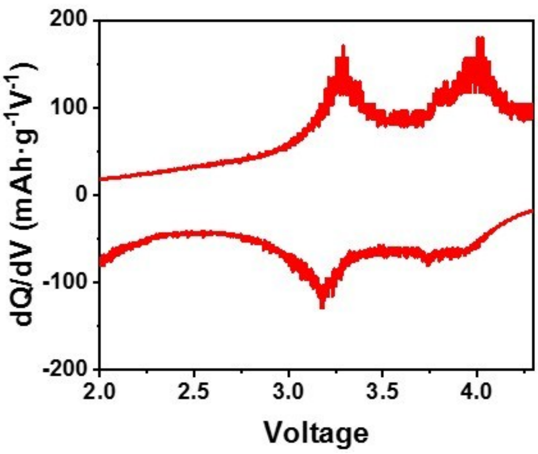

Fig. S10. dQ/dV curve of a cell cycled in 1.5-4.5 V under the current density of 120 mA g^{-1}, corresponding to GCD curve in Figure 2a.

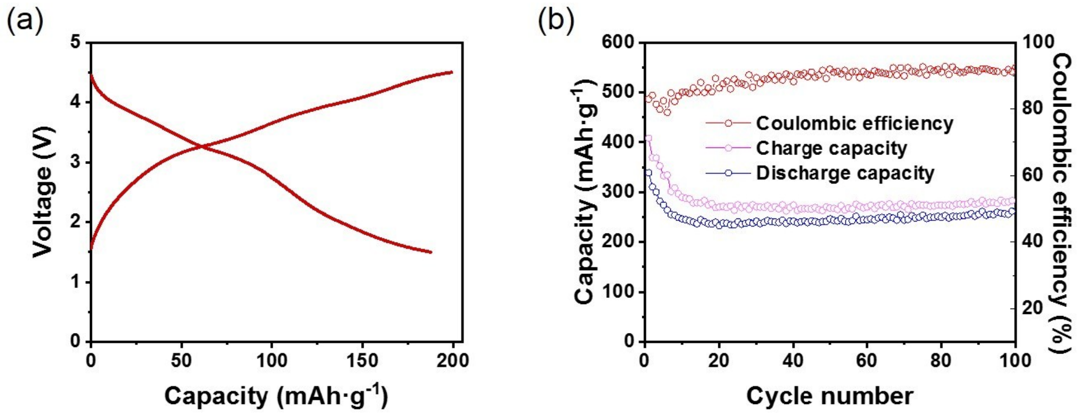

Fig. S11. The GCD curve and cycle stability of a cell under the current density of 25 mA g^{-1}.

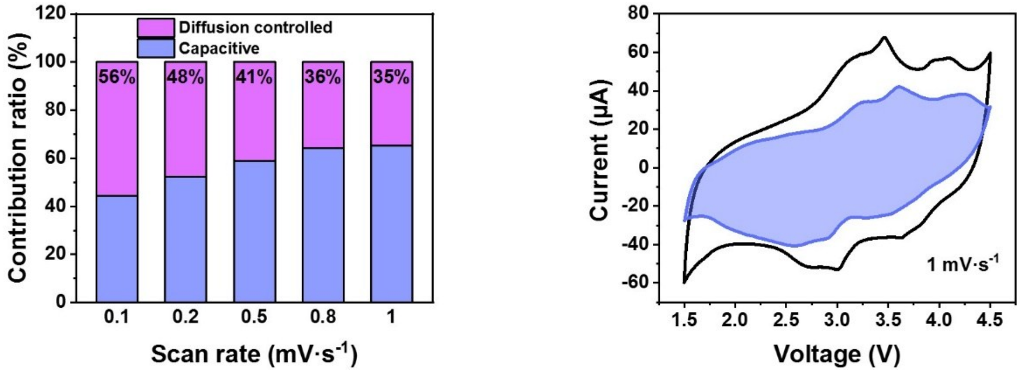

Fig. S12. Dynamic analysis. (a) Specific percentages of diffusion control at different scan rates. (b) Schematic illustration of capacitance-process (blue) at 1 mV s^{-1}.

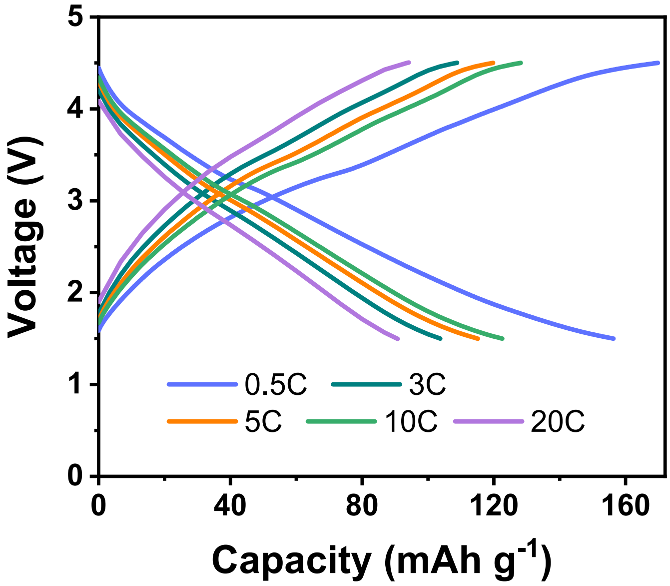

Fig. S13. GCD curves at different current densities. 1C = 120 mAg^{-1}.

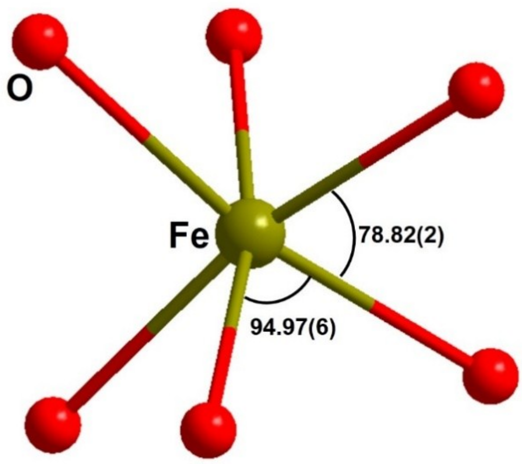

Fig. S14. Motif of [FeO_6] octahedron with maximun and minimum bond angles highlighted.

Table S1. Rietveld refinement of pristine $KLi_3Fe(C_2O_4)_3$.

Trigonal system, ***R -3c*** (No. 167), Mr = **379.83** (g/mol), Z = **6**

a = **11.430(1) Å**, *b* = **11.430(1) Å**, *c* =**15.153(1) Å**, V = **1714.5(4)** $Å^3$

Rw **= 0.0786,** wRp **= 0.1027,** CHI^2 **= 1.535**

Atom	**x/a**	**y/b**	**z/c**	**Multiplicity**	U_{iso}
Fe	0	0	0.25	6	0.0288
K1	0.6667	0.3333	0.3333	6	0.0534
O1	0.3939	0.3072	0.3141	36	0.0394
O2	0.1851	0.1108	0.0.3193	36	0.0128
C1	0.2972	0.2149	0.2976	36	0.0115
Li1	0.2228	0.2228	0.25	18	0.0456

Table S2. Assignments of peaks in FTIR and Raman spectra of the pristine sample.

Peaks number	IR	Raman	Band assignments
1	1667(strong)		νa (C=O)
2	1631(strong)		νs (C-O) + ν(C-C)
3	1479(strong)		νs (C-O) + δ(O-C=O)
4	1425		νs (C-O) + δ(O-C=O)
5	1345(strong)		νs (C-O)
6	1319(strong)		δ(O-C=O)
7	912		νs (C-O) + δ(O-C=O)
8	860		δ(O-C=O)
9	804(strong)		ν(M-O)
10	605		ν(M-O) + ν(C-C)
11	480 (strong)		Ring deform + δ(O-C=O)
i		1719	ν (CO)
ii		1645(m)	ν (CO)
iii		1625	ν (CO)
iv		1481(s)	ν (C=O) stretching
v		912(m)	ν (C-C) stretching
vi		851	δ(O-C=O) bending
vii		601	δ(O-C=O) symmetric bending
viii		508(m)	ν (MO ring)

Table S3. Fitting parameters of Fe K-edge EXAFS spectrum of pristine KLFO sample.

Path	Coordination Number	R	S_0^2	ΔE_0 (eV)	σ^2 (Å^2)	*R factor*
Fe-O1	6	2.12(4)	0.71	2.982	0.01	0.019
Fe-C	6	2.87(4)	0.71	2.982	0.01	
Fe-O1-C	12	3.13(4)	0.71	2.982	0.01	
Fe-O2	6	4.08(11)	0.71	2.982	0.01	
Fe-C-O2	12	4.09(5)	0.71	2.982	0.01	

Table S4 Quantitative analysis of the oxidation state by linear combination fitting of Fe *K*-edge XANES.

Time	**E (eV)**	**ΔE (eV)**	**oxidation state**	**%Fe^{3+}**	**%Fe^{2+}**
Ref Fe^{2+}	7121.80	0.00	2.000	0	100
Ref Fe^{3+}	7126.80	5.00	3.000	100	0
20	7122.05	0.25	2.05	5	95
30	7122.42	0.62	2.124	12.4	87.6
40	7122.42	0.62	2.124	12.4	87.6
50	7122.49	0.69	2.138	13.8	86.2
60	7122.53	0.73	2.146	14.6	85.4
70	7122.61	0.81	2.162	16.2	83.8
80	7122.65	0.85	2.17	17	83
90	7122.9	1.1	2.22	22	78
100	7122.99	1.19	2.238	23.8	76.2
110	7123.72	1.92	2.384	38.4	61.6
120	7123.97	2.17	2.434	43.4	56.6
130	7124.44	2.64	2.528	52.8	47.2
140	7124.92	3.12	2.624	62.4	37.6
150	7125.37	3.57	2.714	71.4	28.6
160	7126.01	4.21	2.842	84.2	15.8
170	7126.75	4.95	2.99	99	1
180	7126.59	4.79	2.958	95.8	4.2
190	7125.83	4.03	2.806	80.6	19.4
200	7125.69	3.89	2.778	77.8	22.2
210	7125.07	3.27	2.654	65.4	34.6
220	7124.43	2.63	2.526	52.6	47.4
230	7124.18	2.38	2.476	47.6	52.4
240	7123.47	1.67	2.334	33.4	66.6
250	7123.05	1.25	2.25	25	75
260	7122.96	1.16	2.232	23.2	76.8
270	7122.63	0.83	2.166	16.6	83.4
280	7122.62	0.82	2.164	16.4	83.6
290	7122.54	0.74	2.148	14.8	85.2
300	7122.5	0.7	2.14	14	86
310	7122.44	0.64	2.128	12.8	87.2
320	7122.4	0.6	2.12	12	88
330	7122.31	0.51	2.102	10.2	89.8
340	7122	0.2	2.04	4	96

Table S5. Electrochemical performances of KLFO@C and cathode materials of recently reported for potassium-ion devices.

Cathode material	Type	Voltage [V]	Current density (mA g⁻¹)	Stable capacity	Cycle number	Capacity after cycles (mA g⁻¹)	Ref.
P2-type $K_{2/3}Ni_{1/3}Co_{1/3}Te_{1/3}O_2$	oxide	1.25–5.0	6.5	30	25	30	6
P2-Type $K_{0.65}Fe_{0.5}Mn_{0.5}O_2$	oxide	1.5–4.2	100	103	350	80	7
P2-type $Na_{0.84-x}K_xCoO_2$	oxide	2.0–4.2	7.6	82	50	69	8
P2-type $K_2Ni_2TeO_6$	oxide	1.3–4.7	6	70	70	62	9
P2-Type $K_{0.6}CoO_2$	oxide	1.7–4.0	100	62	120	37	9
P2-type $K_{0.6}CoO_2$	oxide	1.7–4.0	40	75	300	65	10
P3-type $K_{0.45}MnO_2$	oxide	1.5−4.0	20	101	100	66.7	11
P′2-type $K_{0.3}MnO_2$	oxide	1.5–3.5	28	74	700	50	12
P2-type $K_{0.41}CoO_2$	oxide	2.0–3.9	11.8	57	30	54	12
P3-type $K_{2/3}CoO_2$	oxide	2.0–3.9	11.8	60	30	55	13
P3-$K_{0.69}CrO_2$	oxide	1.5–3.8	100	100	1000	65	14
P3-$K_{0.8}CrO_2$	oxide	1.5-3.9	10	90	300	50	15
P3-Type $K_{0.5}MnO_2$	oxide	1.5–4.2	5	140	20	49	16
P3-Type $K_{0.5}MnO_2$	oxide	1.5–3.9	5	110	20	86	17
P3-$K_{0.54}[Co_{0.5}Mn_{0.5}]O_2$	oxide	1.5−4.0	500	78	500	48	18
P′3-type $Na_{0.52}CrO_2$	oxide	2.0−3.6	500	52	200	51	19
O3-type $KCrS_2$	oxide	1.8–3.0	9	71	1000	64	20
O3-type $KCrO_2$	oxide	1.5–4.0	10	85	100	57	21
$K_{0.37}Na_{0.3}Ni_{0.17}Co_{0.17}Mn_{0.66}O_2$	oxide	2.0–4.2	20	86.1	100	78.8	22
$K_{0.67}Ni_{0.17}Co_{0.17}Mn_{0.66}O_2$	oxide	2.0–4.3	20	80	100	72	23
$K_{0.7}Fe_{0.5}Mn_{0.5}O_2$	oxide	1.5–4.0	20	178	45	125	24
$K_{1.06}Mn_8O_{16}$/CNT	oxide	1.5−4.0	500	125	100	72.2	25
$V_2O_5\cdot 0.6H_2O$	oxide	1.5−4.0	50	155	500	103	26
$K_xV_2O_5\cdot nH_2O$	oxide	2.0–4.3	20	226	50	167	27
$K_{0.77}MnO_2\cdot 0.23H_2O$	oxide	1.5−4.0	1000	77	1000	62	28
$K_{0.32}MnO_2$	oxide	2.0–4.5	100	49.2	100	36.1	29
$Na_{0.9}Cr_{0.9}Ru_{0.1}O_2$	oxide	1.5–3.8	500	62	500	50.3	30
$K_xMnO_2\cdot nH_2O$	oxide	1.5–4.0	80	86	50	68	31
$K_{0.45}Mn_{0.9}Mg_{0.1}O_2$	oxide	1.5-4.0	20	108	100	80.8	32
$K_{0.28}MnO_2\cdot 0.15H_2O$	oxide	1.4-3.6	152	0.1C	100	123	33
AlF_3@ $K_{1.39}Mn_3O_6$	oxide	1.5−4.0	10	110	100	105	34
$K_{0.5}V_2O_5$	oxide	1.0–3.0	100	60	250	49	35
$K_2V_3O_8$/C	oxide	1.0–4.2	20	75	200	60	36
V_2O_5	oxide	2.0–4.5	100	77.8	100	48	37
V_2O_5@rGO	oxide	1.5−4.3	147	222	500	178	38
V_2O_5@CNT	oxide	1.5-3.8	5	150	50	80	39
$H_2V_3O_8$	oxide		5	168	100	126	40
$K_{0.486}V_2O_5$	oxide	1.5-4.2	20	159	100	44.3	41
$KFeO_2$	oxide	1.7-3.7	10	60	50	30	42
$KMn_{7.6}Co_{0.4}O_{16}$	oxide	1.5-4.0	100	174	50	75	43
$KNi_{1/3}Mn_{2/3}O_2$	oxide	1.5-4.5	86	82	200	73	44
$K_{0.3}Ti_{0.75}Fe_{0.25}[Fe(CN)_6]_{0.95}\cdot 2.8H_2O$	PBAs	1.0–4.5	100	113	100	73.1	45
$K_{0.220}Fe[Fe(CN)_6]_{0.805}\cdot 4.01H_2O$	PBAs	2.0–4.0	50	74.5	50	73.2	46
$K_{1.6}Mn[Fe(CN)_6]_{0.96}\cdot 0.27H_2O$	PBAs	3.2–4.3	50	110	30	86	47
$K_{1.70}Mn[Fe(CN)_6]_{0.90}\cdot 1.10H_2O$	PBAs	2.5–4.6	156	110	100	100	48
$K_{1.75}Mn[Fe(CN_6)]_{0.93}\cdot 0.16H_2O$	PBAs	2.0–4.5	30	120	100	116	47
$K_{1.89}Mn[Fe(CN_6)]_{0.92}\cdot 0.75H_2O$	PBAs	2.5-4.6	0.2C	142.4			49
$K_{1.64}Fe[Fe(CN)_6]_{0.89}\cdot 0.15H_2O$	PBAs	2.0–4.5	30	122	100	110	50
$K_{1.88}Zn_{2.88}[Fe(CN)_6]_2(H_2O)_5$	PBAs	3.4−4.15	14	55.6	100	52.8	51

$K_{1.92}Fe[Fe(CN)_6]_{0.94}\cdot 0.5H_2O$	PBAs	2.0–4.3	13	133	200	123	52
$K_{1.7}Fe[Fe(CN)_6]_{0.9}$	PBAs	2.0–4.5	100	120	300	78	53
$K_{1.59}Fe_{2.20}(CN)_6$	PBAs	2.25–4.25	77.5	148	1000	99	53
$K_{1.68}Fe_{1.09}[Fe(CN)_6]\cdot 2.1H_2O$	PBAs	2.0-4.5	20	110	100	81	53
$K_{1.55}Co_{0.88}[Fe(CN)_6]\cdot 3.2H_2O$	PBAs	2.0-4.5	20	60	15	38.4	53
$K_{1.51}Ni_{1.05}[Fe(CN)_6]\cdot 2.1H_2O$	PBAs	2.0-4.5	20	63	15	58.6	54
$K_{1.40}Cu_{0.93}[Fe(CN)_6]\cdot 2.1H_2O$	PBAs	2.0-4.5	20	36	15	30	55
$KFe[Fe(CN)_6]$	PBAs	2.0–4.5	100	90.7	1000	73	56
$KFe[Fe(CN)_6]$	PBAs	0.8–2.1	2000	72	50	58	57
$KFe^{3+}[Fe^{2+}(CN)_6]$	PBAs	2.5–4.2	8.7	78	500	69	58
$K_{1.85}Mn[Fe(CN_6)]_{0.98}\cdot 0.7H_2O$	PBAs	2.0-4.5	15	126	120	120.1	59
$K_{1.81}Mn[Fe(CN_6)]_{0.97}\cdot 0.086H_2O$	PBAs PBAs	2.0-4.5	10	57	1000	50	60
$K_{1.4}Fe_4[Fe(CN)_6]_3$	PBAs	2.0-4.0	50	72	40	57.6	61
$K_{1.62}Fe[Fe(CN)_6]_{0.92}0.33H_2O$	PBAs	2.5-4.5	50	120.9	100	117	62
5% Ni-doped PB	PBAs	2.0-4.2	100	135	300	112	63
RGO@PB@SSM	PBAs	2.0–4.0	50	61.4	305	46	64
KHCF@PPy	PBAs	2.0–4.2	50	88.8	500	77.1	65
$K_2FeFe(CN)_6$	PBAs	2.0–4.3	20	110	100	89	66
$FeFe(CN)_6$	PBAs	0.0–0.975	111	140	20	119	67
$K_4Fe(CN)_6$	PBAs	2.0–3.8	20	65.5	400	48.8	68
$FeFe(CN)_6$	PBAs	1.5–4.0	625	100	500	93	69
o-$Na_2C_6H_2O_6$	Organic	1.0–3.0	25	98.8	100	65.1	70
p-$Na_2C_6H_2O_6$	Organic	1.0–3.0	25	228.5	50	190	71
CuTCNQ	Organic	2.0–4.0	50	206	50	170	72
HAT-containing polymer	Organic	0.9-3.4	10000	150	4500	150	73
PTCDA	Organic	1.5–3.5	50	117	200	90	74
PTCDA	Organic	1.2–3.2	10	87	300	63	75
PTCDA	Organic	1.5–3.5	1000	113	1000	98	76
AQDS	Organic	1.4–3.0	13	95	100	78	77
AQDS	Organic	1.4–3.0	390	80	1000	64	78
PAQS	Organic	1.5–3.4	200	106	200	68	79
PTPAn	Organic	2.0−4.0	100	75	60	71	80
PVK	Organic	2.0–4.7	500	104	400	73	81
PAN	Organic	2.0−4.0	50	100	100	98	82
SR	Organic	1.5–3.8	125	118	100	82	83
PQ-1, 5	Organic	1.2–3.2 V	250	115	200	105	84
PI-CMP	Organic	1.5–3.5 V	1000	109	1000	80.8	85
PPTS	Organic	0.8-3.2	100	282.3	-	-	86
p-DPPZ	Organic	2.5-4.5	162	200	1000	120	87
$Na_2AQ_{26}DS$	Organic	1.5-3.7	100	105	200	105	88
OHTAP	Organic	1.1-2.8	0.1C	220	50	162	89
Polydiaminoanthraquinone	Organic	1.2–3.2	250	120	200	105	90
PI@G	Organic	1.4-3.5	100	142	500	118	91
PTCDI	Organic	1.4-3.8	100	157	600	120	92
$K_2[(VO)_2(HPO_4)_2(C_2O_4)]$	Polyanion	2.0–4.6	22	65	200	54	93
$VOPO_4\cdot 2H_2O$	Polyanion	-0.2–1.3	27	88.3	100	76	93
$FePO_4$	Polyanion	1.5-3.5	5	156	50	134	94
$K_3V_2(PO_4)_3/C$	Polyanion	2.5–4.3	20	55	100	52	95
$KTi_2(PO_4)_3/C$	Polyanion	1.2–2.8	64	75.6	100	82	96
$KVPO_4F$	Polyanion	2.0–4.8	6.65	72	50	65	96
$KVOPO_4$	Polyanion	2.0–4.8	6.65	73	50	69	96
$KVOPO_4$	Polyanion		24	115	100	60	97
$KVPO_4F$	Polyanion	3.0–5.0	5	100	30	78	98
KVP_2O_7	Polyanion	2.0–5.0	25	60	100	51	99
$KMoP_2O_7$	Polyanion	2.0–5.0	1C	25	-	-	100
$KTiP_2O_7$	Polyanion	2.0–5.0	1C	22	-	-	101
$K_3V_2(PO_4)_3$	Polyanion	0.01–3.0	25	88	500	78	102
$K_3V_2(PO_4)_2F_3$	Polyanion	2.0–4.5	10	101	100	98	103
K(Mn,Co)F3	Others	1.2–4.2	40	132.6	60	103.4	104
I_2	Others	1.9–3.5	100	115	500	82	105
KLFO@C	**Polyanion**	**1.5–4.5**	**120**	**140**	**5000**	**130**	**This**

References

(1) Masese, T. *et al.* A high voltage honeycomb layered cathode framework for rechargeable potassium-ion battery: P2-type $K_{2/3}Ni_{1/3}Co_{1/3}Te_{1/3}O_2$. *Chem. Commun.* **55**, 985-988 (2019).

(2) Deng, T. *et al.* Layered P2-Type $K_{0.65}Fe_{0.5}Mn_{0.5}O_2$ Microspheres as Superior Cathode for High-Energy Potassium-Ion Batteries. *Adv. Funct. Mater.* **28**, 1800219 (2018).

(3) Sada, K., Senthilkumar, B. & Barpanda, P. Electrochemical potassium-ion intercalation in Na_xCoO_2: a novel cathode material for potassium-ion batteries. *Chem. Commun.* **53**, 8588-8591 (2017).

(4) Masese, T. *et al.* Rechargeable potassium-ion batteries with honeycomb-layered tellurates as high voltage cathodes and fast potassium-ion conductors. *Nat. Commun.* **9**, 3823 (2018).

(5) Kim, H. *et al.* K-Ion Batteries Based on a P2-Type $K_{0.6}CoO_2$ Cathode. *Adv. Energy Mater.* **7**, 1700098 (2017).

(6) Deng, T. *et al.* Self-Templated Formation of P2-type $K_{0.6}CoO_2$ Microspheres for High Reversible Potassium-Ion Batteries. *Nano Lett.* **18**, 1522-1529 (2018).

(7) Liu, C.-L., Luo, S.-H., Huang, H.-B., Zhai, Y.-C. & Wang, Z.-W. Layered potassium-deficient P2- and P3-type cathode materials K_xMnO_2 for K-ion batteries. *Chem. Eng. J.* **356**, 53-59 (2019).

(8) Vaalma, C., Giffin, G. A., Buchholz, D. & Passerini, S. Non-Aqueous K-Ion Battery Based on Layered $K_{0.3}MnO_2$ and Hard Carbon/Carbon Black. *J. Electrochem. Soc.* **163**, A1295-A1299 (2016).

(9) Hironaka, Y., Kubota, K. & Komaba, S. P2- and P3-K_xCoO_2 as an electrochemical potassium intercalation host. *Chem. Commun.* **53**, 3693-3696 (2017).

(10) Hwang, J.-Y., Kim, J., Yu, T.-Y., Myung, S.-T. & Sun, Y.-K. Development of P3-$K_{0.69}CrO_2$ as an ultra-high-performance cathode material for K-ion batteries. *Energy Environ. Sci.* **11**, 2821-2827 (2018).

(11) Naveen, N., Han, S., Singh, S., Ahn, D., Sohn, K.-S., Pyo, M., Highly stable P_3-$K_{0.8}CrO_2$ cathode with limited dimensional changes for potassium ion batteries. *J. Power Sources* **430**, 137–144 (2019).

(12) Kim, H. *et al.* Investigation of Potassium Storage in Layered P3-Type $K_{0.5}MnO_2$ Cathode. *Adv. Mater.* **29** 1702480 (2017).

(13) Choi, J. *et al.* $K_{0.54}[Co_{0.5}Mn_{0.5}]O_2$: New cathode with high power capability for potassium-ion batteries. *Nano Energy* **61**, 284-294 (2019).

(14) Naveen, N. *et al.* Reversible K^+-Insertion/Deinsertion and Concomitant Na^+-Redistribution in P′3-$Na_{0.52}CrO_2$ for High-Performance Potassium-Ion Battery Cathodes. *Chem. Mater.* **30**, 2049-2057 (2018).

(15) Naveen, N. *et al.* $KCrS_2$ Cathode with Considerable Cyclability and High Rate Performance: The First K^+ Stoichiometric Layered Compound for Potassium-Ion Batteries. *Small* **14**, 1803495 (2018).

(16) Kim, H. *et al.* Stoichiometric Layered Potassium Transition Metal Oxide for Rechargeable Potassium Batteries. *Chem. Mater.* **30**, 6532-6539 (2018).

(17) Liu, C.-L., Luo, S.-H., Huang, H.-B., Zhai, Y.-C. & Wang, Z.-W. Influence of Na-substitution on the structure and electrochemical properties of layered oxides $K_{0.67}Ni_{0.17}Co_{0.17}Mn_{0.66}O_2$ cathode materials. *Electrochim. Acta* **286**, 114-122 (2018).

(18) Liu, C. *et al.* $K_{0.67}Ni_{0.17}Co_{0.17}Mn_{0.66}O_2$: A cathode material for potassium-ion battery. *Electrochem. Commun.* **82**, 150-154 (2017).

(19) Wang, X. *et al.* Earth Abundant Fe/Mn-Based Layered Oxide Interconnected Nanowires for Advanced K-Ion Full Batteries. *Nano Lett.* **17**, 544-550 (2017).

(20) Chong, S. *et al.* Cryptomelane-type MnO_2/carbon nanotube hybrids as bifunctional electrode material for high capacity potassium-ion full batteries. *Nano Energy* **54**, 106-115 (2018).

(21) Tian, B., Tang, W., Su, C. & Li, Y. Reticular $V_2O_5{\cdot}0.6H_2O$ Xerogel as Cathode for Rechargeable Potassium Ion Batteries. *ACS Appl. Mater. Interfaces* **10**, 642-650 (2018).

(22) Clites, M., Hart, J. L., Taheri, M. L. & Pomerantseva, E. Chemically Preintercalated Bilayered $K_xV_2O_5{\cdot}nH_2O$ Nanobelts as a High-Performing Cathode Material for K-Ion Batteries. *ACS Energy Lett.* **3**, 562-567 (2018).

(23) Lin, B. *et al.* Birnessite Nanosheet Arrays with High K Content as a High-Capacity and Ultrastable Cathode for K-Ion Batteries. *Adv. Mater.* **31**, 1900060 (2019).

(24) Chong, S. *et al.* Mn-based layered oxide microspheres assembled by ultrathin nanosheets as cathode material for potassium-ion batteries. *Electrochim. Acta* **293**, 299-306 (2019).

(25) Zhang, H. *et al.* Enhanced K-ion kinetics in a layered cathode for potassium ion batteries. *Chem. Commun.* DOI:10.1039/c9cc03156a (2019).

(26) Gao, A. *et al.* K-Birnessite Electrode Obtained by Ion Exchange for Potassium-Ion Batteries: Insight into the Concerted Ionic Diffusion and K Storage Mechanism. *Adv. Energy Mater.* **9**, 1802739 (2019).

(27) Liu, C-L., Luo, S., Huang, H., Zhai, Y., & Wang, Z., Low-Cost Layered $K_{0.45}Mn_{0.9}Mg_{0.1}O_2$ as a High-Performance Cathode Material for K-Ion Batteries. *ChemElectroChem* **6**, 2308–2315 (2019).

(28) Jo, J., Hwang, J.Y., Choi, J., Sun, Y.-K., & Myung, S.-T., Layered $K_{0.28}MnO_2{\cdot}0.15H_2O$ as a Cathode Material for Potassium-Ion Intercalation, *ACS Appl. Mater. Interfaces* DOI: 10.1021/acsami.9b18540.(2019)

(29) Zhao, S., Yan, K., Munroe, P., Sun, B. & Wang, G. Construction of Hierarchical $K_{1.39}Mn_3O_6$ Spheres via AlF_3 Coating for High-Performance Potassium-Ion Batteries. *Adv. Energy Mater.* **9**, 1803757 (2019).

(30) Deng, L. *et al.* Layered Potassium Vanadate $K_{0.5}V_2O_5$ as a Cathode Material for Nonaqueous Potassium Ion Batteries. *Adv. Funct. Mater.* **28**, 1800670 (2018).

(31) Jo, J. *et al.* Potassium vanadate as a new cathode material for potassium-ion batteries. *J. Power Sources* **432**, 24-29 (2019).

(32) Zhu, Y.-H. *et al.* Reconstructed Orthorhombic V_2O_5 Polyhedra for Fast Ion Diffusion in K-Ion Batteries. *Chem* **5**, 168-179 (2019).

(33) Vishnuprakash, P., Nithya, C. & Premalatha, M. Exploration of V_2O_5 nanorod@rGO heterostructure as potential cathode material for potassium-ion batteries. *Electrochim. Acta* **309**, 234-241 (2019).

(34) Yuan, K. *et al*. Prepotassiated V_2O_5 as the Cathode Material for High-Voltage Potassium-Ion Batteries. *Energy Technol.* 1900796 (2019).

(35) Mohadese, R., Jongwook, W. H., & Hong, S.-T., High Potassium Storage Capability of $H_2V_3O_8$ in a NonAqueous Electrolyte, *ChemistrySelect*, **4**, 11711–11717 (2019).

(36) Ye, F., Lu, D., Gui, X., Wang, T., Zhuang, X., Luo, W., Huang, Y. Atomic layer deposition of core-shell structured V_2O_5@CNT sponge as cathode for potassium ion batteries. *J. Materiomics* **5**, 344-349 (2019).

(37) Han, S., Park, W., Sohn, K.-S. & Pyo, M., $KFeO_2$ with corner-shared FeO_4 frameworks as a new type of cathode material in potassium-ion batteries. *J Solid State Electrochem* **23**, 3135–3143 (2019).

(38) Tai, Z. *et al*. $KMn_{7.6}Co_{0.4}O_{16}$ nano-rod clusters with a high discharge specific capacity as cathode materials for potassium-ion batteries, *Sus.EngeryFuels* 2019, 10.1039/C8SE00550H.

(39) Nathan, M., Naveen, N., Park, W., Sohn, K.-S., Pyo, M., Fast chargeable P2–$K_{\sim 2/3}[Ni_{1/3}Mn_{2/3}]O_2$ for potassium ion battery cathodes. *J. Power Sources* **438**, 226992 (2019).

(40) Luo, Y. *et al.* Potassium titanium hexacyanoferrate as a cathode material for potassium-ion batteries. *J. Phys. Chem. Solids* **122**, 31-35 (2018).

(41) Zhang, C. *et al.* Potassium Prussian Blue Nanoparticles: A Low-Cost Cathode Material for Potassium-Ion Batteries. *Adv. Funct. Mater.* **27**, 1604307 (2017).

(42) Jiang, X., Zhang, T., Yang, L., Li, G. & Lee, J. Y. A Fe/Mn-Based Prussian Blue Analogue as a K-Rich Cathode Material for Potassium-Ion Batteries. *ChemElectroChem* **4**, 2237-2242 (2017).

(43) Xue, L. *et al.* Low-Cost High-Energy Potassium Cathode. *J Am. Chem. Soc.* **139**, 2164-2167 (2017).

(44) Bie, X., Kubota, K., Hosaka, T., Chihara, K. & Komaba, S. A novel K-ion battery: hexacyanoferrate(ii)/graphite cell. *J. Mater. Chem. A* **5**, 4325-4330 (2017).

(45) Xue, L. G., Li, Y. T., Gao, H. C., Zhou, W. D., Lu, X. J. Kaveevivitchai, W., Manthiram, A. & Goodenough, J.B., Low-cost high-energy potassium cathode, *J. Am. Chem. Soc.* **139**, 2164–2167 (2017).

(46) Heo, J. W., Chae, M. S., Hyoung, J. & Hong, S. T. Rhombohedral Potassium-Zinc Hexacyanoferrate as a Cathode Material for Nonaqueous Potassium-Ion Batteries. *Inorg. Chem.* **58**, 3065-3072 (2019).

(47) Liao, J. *et al.* A potassium-rich iron hexacyanoferrate/dipotassium terephthalate@carbon nanotube composite used for K-ion full-cells with an optimized electrolyte. *J. Mater. Chem. A* **5**, 19017-19024 (2017).

(48) He, G. & Nazar, L. F. Crystallite Size Control of Prussian White Analogues for Nonaqueous Potassium-Ion Batteries. *ACS Energy Lett.* **2**, 1122-1127 (2017).

(49) Piernas-Muñoz, M. J., Castillo-Martínez, E., Bondarchuk, O., Armand, M. & Rojo, T. Higher voltage plateau cubic Prussian White for Na-ion batteries. *J. Power Sources* **324**, 766-773 (2016).

(50) He, G., Nazar, L.F. Crystallite size control of Prussian white analogues for nonaqueous potassium-ion batteries, *ACS Energy Lett* **5**, 1122–1127 (2017).

(51) Chong, S. *et al.* Potassium ferrous ferricyanide nanoparticles as a high capacity and ultralong life cathode material for nonaqueous potassium-ion batteries. *J. Mater. Chem. A* **5**, 22465-22471 (2017).

(52) Wang, J. *et al.* A bi-functional device for self-powered electrochromic window and self-rechargeable transparent battery applications. *Nat. Commun.* **5**, 4921 (2014).

(53) Eftekhari, A. Potassium secondary cell based on Prussian blue cathode. *J. Power Sources* **126**, 221-228 (2004).

(54) Sun, Y., Liu, C., Xie, J., Zhuang, D., Zheng W. & Zhao, X. Potassium manganese hexacyanoferrate/grapheme as a high-performance cathode for potassium-ion batteries. *New J. Chem.* **43**, 11618 (2019).

(55) Chong, S., Wu, Y., Guo, S., Liu, Y., Cao, G., Potassium nickel hexacyanoferrate as cathode for high voltage and ultralong life potassium-ion batteries. *Energy Storage Materials* **22**, 120–127 (2019).

(56) Qin, M., Ren, W., Meng, J., Wang, X., Yao, X., Ke, Y., Li, Q. & Mai, L. Realizing Superior Prussian Blue Positive Electrode for Potassium Storage via Ultrathin Nanosheet Assembly. *ACS Sustainable Chem. Eng.* **7**, 11564-11570 (2019).

(57) Dong, J., Lei, Y., Han, D., Wang, H., Zhai, D., Li B., & Kang F., Utilizing an autogenously protective atmosphere to synthesize a Prussian white cathode with ultrahigh capacity-retention for potassium-ion batteries. *Chem. Commun.* **55**, 12555 (2019).

(58) Huang, B., Liu, Y., Lu, Z., Shen, M., Zhou, J., Ren, J., Li, X. & Liao, S. Prussian Blue [$K_2FeFe(CN)_6$] Doped with Nickel as a Superior Cathode: An Efficient Strategy To Enhance Potassium Storage Performance. *ACS Sustainable Chem. Eng.* **7**, 16659-16667 (2019).

(59) Zhu, Y. H. *et al.* Transformation of Rusty Stainless-Steel Meshes into Stable, Low-Cost, and Binder-Free Cathodes for High-Performance Potassium-Ion Batteries. *Angew. Chem. Int. Ed.* **56**, 7881-7885 (2017).

(60) Xue, Q. *et al.* Polypyrrole-Modified Prussian Blue Cathode Material for Potassium Ion Batteries via In Situ Polymerization Coating. *ACS Appl. Mater. Interfaces* **11**, 22339-22345 (2019).

(61) Wu, X., Jian, Z., Li, Z. & Ji, X. Prussian white analogues as promising cathode for non-aqueous potassium-ion batteries. *Electrochem. Commun.* **77**, 54-57 (2017).

(62) Padigi, P. *et al.* Prussian Green: A High Rate Capacity Cathode for Potassium Ion Batteries. *Electrochim. Acta* **166**, 32-39 (2015).

(63) Pei, Y., Mu, C., Li, H., Li, F. & Chen J. Low-Cost $K_4Fe(CN)_6$ as aHigh-Voltage Cathode for Potassium-Ion Batteries. *ChemSusChem* **11**, 1285-1289 (2018).

(64) Shadike, Z. *et al.* Long life and high-rate Berlin green $FeFe(CN)_6$ cathode material for a non-aqueous potassium-ion battery. *J. Mater. Chem. A* **5**, 6393-6398 (2017).

(65) Chen, L. *et al.* Ortho-di-sodium salts of tetrahydroxyquinone as a novel electrode for lithium-ion and potassium-ion batteries. *Electrochim. Acta* **294**, 46-52 (2019).

(66) Chen, L. & Zhao, Y. Exploration of *p*-$Na_2C_6H_2O_6$-based organic electrode materials for sodium-ion and potassium-ion batteries. *Mater. Lett.* **243**, 69-72 (2019).

(67) Ma, J. *et al.* Endowing CuTCNQ with a new role: a high-capacity cathode for K-ion batteries. *Chem. Commun.* **54**, 5578-5581 (2018).

(68) Kapaev, R., Zhidkov, I., Kurmaev, E., Stevenson K. & Troshin, P. Hexaazatriphenylene-based polymer cathode for fast and stable lithium-, sodium- and potassiumion batteries. *J. Mater. Chem. A* **7**, 22596 (2019).

(69) Chen, Y. *et al.* Organic electrode for non-aqueous potassium-ion batteries. *Nano Energy* **18**, 205-211 (2015).

(70) Xing, Z. *et al.* A perylene anhydride crystal as a reversible electrode for K-ion batteries. *Energy Storage Mater.* **2**, 63-68 (2016).

(71) Fan, L., Ma, R., Wang, J., Yang, H. & Lu, B. An Ultrafast and Highly Stable Potassium-Organic Battery. *Adv. Mater.* **30**, 1805486 (2018).

(72) Zhao, J., Yang, J., Sun, P. & Xu, Y. Sodium sulfonate groups substituted anthraquinone as an organic cathode for potassium batteries. *Electrochem. Commun.* **86**, 34-37 (2018).

(73) Li, B. *et al.* Electrolyte-Regulated Solid-Electrolyte Interphase Enables Long Cycle Life Performance in Organic Cathodes for Potassium-Ion Batteries. *Adv. Funct. Mater.* **29**, 1807137 (2018).

(74) Jian, Z., Liang, Y., Rodríguez-Pérez, I. A., Yao, Y. & Ji, X. Poly(anthraquinonyl sulfide) cathode for potassium-ion batteries. *Electrochem. Commun.* **71**, 5-8 (2016).

(75) Fan, L., Liu, Q., Xu, Z. & Lu, B. An Organic Cathode for Potassium Dual-Ion Full Battery. *ACS Energy Lett.* **2**, 1614-1620 (2017).

(76) Li, C. *et al.* Poly(N-vinylcarbazole) as an advanced organic cathode for potassium-ion-based dual-ion battery. *Electrochim. Acta* **297**, 850-855 (2019).

(77) Gao, H., Xue, L., Xin, S. & Goodenough, J. B. A High-Energy-Density Potassium Battery with a Polymer-Gel Electrolyte and a Polyaniline Cathode. *Angew. Chem. Int. Ed.* **57**, 5449-5453 (2018).

(78) Ding, Y. *et al.* A Liquid-Metal-Enabled Versatile Organic Alkali-Ion Battery. *Adv. Mater.* **31**, 1806956 (2019).

(79) Zhou, M. *et al.* Polydiaminoanthraquinones with tunable redox properties as high performance organic cathodes for K-ion batteries. *Chem. Commun.* **55**, 6054-6057 (2019).

(80) Tian, B. *et al.* Carbonyl-based polyimide and polyquinoneimide for potassium-ion batteries. *J. Mater. Chem. A* **7**, 9997-10003 (2019).

(81) Tang, M., Wu, Y.C., Chen, Y., Jiang, C., Zhu, S.L., Zhuo, S.M. & Wang, C.L. An organic cathode with high capacities for fast-charge potassium-ion batteries, *J. Mater. Chem.* **7**, 486–492 (2019).

(82) Obrezkov, F. *et al*. High-Energy and High-Power-Density Potassium Ion Batteries Using Dihydrophenazine-Based Polymer as Active Cathode Material. *J. Phys. Chem. Lett.* **10**, 5440-5445 (2019).

(83) Li, D., Tang, W., Wang, C., Fan, C. A polyanionic organic cathode for highly efficient K-ion full batteries, *Electrochem. Commun.* **105**, 106509 (2019).

(84) Slesarenko, A. *et al*. New tetraazapentacene-based redox-active material as a promising high-capacity organic cathode for lithium and potassium batteries. *J. Power Sources* **435**, 226724 (2019).

(85) Zhou, M. *et al*. Polydiaminoanthraquinones with tunable redox properties as high performance organic cathodes for K-ion batteries. *Chem. Commun.* **55**, 6054 (2019).

(86) Hu, Y. *et al*. Rational Design of a Polyimide Cathode for a Stable and High-Rate Potassium-Ion Battery, *ACS Appl. Mater. Interfaces* **11**, 42078-42085 (2019).

(87) Liao, J. *et al.* A vanadium-based metal-organic phosphate framework material $K_2[(VO)_2(HPO_4)_2(C_2O_4)]$ as a cathode for potassium-ion batteries. *Chem. Commun.* **55**, 659-662 (2019).

(88) Hyoung, J., Heo, J. W., Chae, M. S. & Hong, S. T. Electrochemical Exchange Reaction Mechanism and the Role of Additive Water to Stabilize the Structure of $VOPO_4 \cdot 2H_2O$ as a Cathode Material for Potassium-Ion Batteries. *ChemSusChem* **12**, 1069-1075 (2019).

(89) Mathew, V., *et al.* Amorphous iron phosphate: potential host for various charge carrier ions, *NPG Asia Mater.* **6** e138–e147 (2014).

(90) Xiong, M., Tang, W., Cao, B., Yang, C. & Fan, C. A small-molecule organic cathode with fast charge–discharge capability for K-ion batteries. *J. Mater. Chem. A* **7**, 20127 (2019).

(91) Han, J. *et al.* Investigation of $K_3V_2(PO_4)_3/C$ nanocomposites as high-potential cathode materials for potassium-ion batteries. *Chem. Commun.* **53**, 1805-1808 (2017).

(92) Han, J. *et al.* Nanocubic $KTi_2(PO_4)_3$ electrodes for potassium-ion batteries. *Chem. Commun.* **52**, 11661-11664 (2016).

(93) Chihara, K., Katogi, A., Kubota, K. & Komaba, S. $KVPO_4F$ and $KVOPO_4$ toward 4 volt-class potassium-ion batteries. *Chem. Commun.* **53**, 5208-5211 (2017).

(94) Kim, H. *et al*. A New Strategy for High-Voltage Cathodes for K-Ion Batteries: Stoichiometric $KVPO_4F$. *Adv. Energy Mater.* **8**, 1801591 (2018).

(95) Jiaying Liao, Qiao Hu, Bo Che, Xiang Ding, Fei Chen and Chunhua Chen, Competing with other polyanionic cathode materials for potassium-ion batteries via fine structure design: new layered KVOPO4 with a tailored particle morphology J. Mater. Chem. A **7**, 15244 (2019)

(96) Park, W. B. *et al.* KVP_2O_7 as a Robust High-Energy Cathode for Potassium-Ion Batteries: Pinpointed by a Full Screening of the Inorganic Registry under Specific Search Conditions. *Adv. Energy Mater.* **8**, 1703099 (2018).

(97) Zhang, L. *et al.* Constructing the best symmetric full K-ion battery with the NASICON-type $K_3V_2(PO_4)_3$. *Nano Energy* **60**, 432-439 (2019).

(98) Lin, X., Huang, J., Tan, H., Huang, J. & Zhang, B. $K_3V_2(PO_4)_2F_3$ as a robust cathode for potassium-ion batteries. *Energy Storage Mater.* **16**, 97-101 (2019).

(99) Wang, S., Cui, B., Zhuang, Q., Shi, Y. & Zheng, H. Synthesis and Electrochemical Performance of Cobalt-Doped $KMnF_3$ as Cathode Materials for Potassium Ion Batteries. *J. Electrochem Soc.* **166**, A1819-A1826 (2019).

(100) Lu, K. *et al.* Rechargeable potassium-ion batteries enabled by potassium-iodine conversion chemistry. *Energy Storage Mater.* **16**, 1-5 (2019).